International Journal of Recent Technology and Engineering (IJRTE)
ISSN: 2277-3878, Volume-8 Issue-3, September 2019

# Understanding of Ice Accumulation and Accretion over an Airfoil

**Swetha S, Abdul Sharief, S. K. Maharana**

***Abstract:*** ***Since the beginning of civil aviation, icing has been a severe weather hazard for aircraft operation. For many years, the term engine icing has been used to describe ice accreting on exposed engine surfaces as an aircraft flies through a cloud of super-cooled liquid droplets. The concern arising out of aircraft icing is due to its adverse effect on flight safety and hence, for decades, a considerable amount of research is on in the area of icing of aircraft and its components exposed to ice. Experimental verification and some of the key numerical investigations in the area have revealed that aerodynamic characteristics and controllability of an aircraft are affected by the amount and type of ice accretion at different locations. Fundamentally icing of airfoil of an aircraft contributes to decrease in lift force as well as the angle of stall on the wing. This also brings up another situation that is longitudinal instability of the apparatus concerned. It has been a complex physical situation to comprehend the accretion process and its impact. In the present study NACA0012 airfoil geometry has been used to understand the accumulation and accretion process through simulation. The results of total mass of ice accreted with respect to total time of accretion (tice) have been presented***

***Keywords: Ice Accretion, Airfoil, RANS, Turbulent Flows, Droplet, Crystal, Viscous Flow.***

## I. INTRODUCTION

The protected aircraft surface is expected to get ice accreted in some typical ridge shape or streak forms (called "barrier" ice). Even though anti-icing equipment and system are fitted to the aircraft, accidents occur primarily due to the presence of overcooled ice droplets. It therefore calls for an investigation of the mechanism that plays role to bring the influence of the "barrier'' ice on the aerodynamics and stability of an aircraft and hence on flight safety. It is necessary to understand the physics of ice accretion before describing further on the reason and the motivation to work further on this crucial topic. Usually there is a rare possibility of detecting high concentration of ice crystals at flight altitude through the radar that is on-board the flight. These crystals are quantified by ice water content (IWC). The quantification is done in a manner similar to liquid water content of super-cooled droplet clouds.

Basically it is the mass of cumulative liquid per unit volume of air surrounding it. As a matter of fact the water drops being formed at high altitude have temperature below 0o C and are overcooled. It is also necessary to dissect the aero hydrodynamic behavior of these water drops through numerical modeling using two-dimensional Reynolds-Averaged Navier–Stokes (RANS) equations.

Some of the outstanding activities and their outcomes in the area of ice accretion were reported in the last decade. The researchers used codes and experimental techniques for their profound understanding and comparison of results. The code ARC2D [4] was written to understand influence of ice accretion on NACA0012 (a standard airfoil by many other researchers as well) on its aerodynamic behavior. The grid used in the flow domain was a structured one and the Navier-Stokes (NS) equations were solved with algebraic two-layer model of turbulence model of Baldwin–Lomax [5]. There was a fairly good agreement between the outputs of numerical experiment in all regions of airfoil except for the region of ice accretion. Subsequently, a study was done to compute ice accretion on the leading edge of an airfoil [6 -7] with the help of RANS in domain meshed with unstructured grids. It was noted that the shape of the ice accretion was a function of the time of accretion which was influenced by external air flow. Another attempt was made on NACA0012 airfoil with adaptable grids with NS equations [8] discretized by Galerkin finite-volume method and the turbulent quantities were modeled using the k–ε model. The Reynolds number was $3.1x10^6$ and Mach number for the study was 0.15.

The objective of the proposed research is to understand and address these issues of ice accretion using a multiphase approach for an airfoil, which is one of the deciding geometric attributes for a fan blade design of a jet-based engine. The geometry considered in the study is a NACA0012 airfoil.

## II. GOVERNING EQUATIONS

Below are given the fundamental equations that are used during the study. These equations are used for the computations of the flow variables using commercially available ANSYS® FANSAP-ICE solver.

Manuscript published on 30 September 2019
* Correspondence Author
**Swetha S**, Assistant Professor, Dept. of Aeronautical Engineering, Acharya Institute of Technology, Bangalore-560107, India. Email: swetha4shree@gmail.com
**Abdul Sharief**, Professor, Dept. of Mechanical Engineering, P.A. College of Engineering, Mangalore-574153, India. Email: abdulsharief2010@gmail.com
**S. K. Maharana**, Professor, Dept. of Aeronautical Engineering, Acharya Institute of Technology, Bangalore-560107, India. Email: saratkumarmaharana@acharya.ac.in

### A. Continuity equation

$$\frac{\partial \rho_a}{\partial t} + \vec{\nabla}.(\rho_a V_a) = 0 \quad (1)$$

Where, ρ is the density and V is the velocity vector. The subscript $^a$ refers to the air solution. This equation is also known as the continuity equation.

### B. Momentum equation

For a Newtonian fluid, Newton second law of motion states that the total force acting on a fluid particle is equal to the time rate of change of its momentum. This can be written in 3D using a set of 3 non-linear equations, shown here in vector form:

$$\frac{\partial \rho_a V_a}{\partial t} + \vec{\nabla}.(\rho_a \vec{V}_a \vec{V}_a) = \vec{\nabla}.\sigma^{ij} + \rho_a \vec{g} \quad (2)$$

Where σij is the stress tensor

$$\sigma^{ij} = -\delta^{ij} p_a + \mu_a \left[\delta^{jk}\nabla_k v^i + \delta^{ik}\nabla_k v^j - \frac{2}{3}\delta^{ij}\nabla_k v^k\right] = -\delta^{ij} p_a + \tau^{ij}$$

$$\tau^{ij} = \mu_a \left[\delta^{jk}\nabla_k v^i + \delta^{ik}\nabla_k v^j - \frac{2}{3}\delta^{ij}\nabla_k v^k\right]$$

p is the static pressure and μ is the dynamic viscosity. The special case of inviscid fluid flows, where the dynamic viscosity is set to zero, yields the Euler equations. For a viscous laminar flow, the viscosity is defined empirically by Sutherland law:

$$\frac{\mu_a}{\mu_\infty} = \left(\frac{T}{T_\infty}\right)^{3/2}\left(\frac{T_\infty + 110}{T + 110}\right)$$

Where, T refers to the static air temperature in Kelvin, and where the subscript ∞ indicates reference values for air: T∞ = 288 K and

μ∞ = 17.9 10-6 Pa s.

### C. Energy equation

The third physical principle concerns the conservation of energy and states that the total energy of the system must be conserved, or:

$$\frac{\partial \rho_a E_a}{\partial t} + \vec{\nabla}.(\rho_a \vec{V}_a \vec{H}_a) = \vec{\nabla}.(\kappa_a(\vec{\nabla}T_a) + v_i \tau^{ij}) + \rho_a \vec{g}.\vec{V}_a \quad (3)$$

Where E and H are the total internal energy and enthalpy, respectively and κ is the thermal conductivity, computed in a similar way to the laminar dynamic viscosity:

$$\kappa = C1 * (T^{\frac{3}{2}})/(T + 133.7)$$

where T refers to the static air temperature in Kelvin, and where the C1 is equal to 0.00216176 W/(mK$^{3/2}$)

## III. APPROACH

Both numerical and experimental approaches have been adopted to solve the problem at hand and substantiate the outcome of the research. The very first approach is to numerically study the ice accumulation and accretion on an airfoil. The icing simulation Messinger model (1953) has been used to derive a three dimensional partial differential equation-based equilibrium equation. The equation is further improved to predict ice accretion and water runback on the surface. In the model, the velocity uf of the water in the film is taken as a function of coordinates x=(x1, x2) on the surface and y normal to the surface. A simplifying assumption consists of taking a linear profile for uf (x,y) with a zero velocity imposed at the wall, i.e.:

$$\mathbf{u}_f(\mathbf{x}, y) = \frac{y}{\mu_w}\tau_{wall}(\mathbf{x}) \quad (4)$$

where $\tau_{wall}$, the shear stress from the air, is the main driving force for the water film. By averaging across the thickness of the film, a mean water film velocity is obtained as given below:

$$\bar{\mathbf{u}}_f(\mathbf{x}) = \frac{1}{h_f}\int_0^{h_f} \mathbf{u}_f(\mathbf{x}, y)dy = \frac{h_f}{2\mu_w}\tau_{wall}(\mathbf{x}) \quad (5)$$

The following equation is used for the mass conservation and energy conservation of the working fluid.

$$\rho_w\left[\frac{\partial h_f}{\partial t} + div\left(\overline{\mathbf{u}}_f h_f\right)\right] = U_\infty LWC\,\beta - \dot{m}_{evap} - \dot{m}_{ice} \quad (6)$$

The terms in the right hand side of the equation (6) are mass transfer (first term) by water droplet impingement (source for the film), evaporation (second term) and ice accretion (third term). The second and third terms are sinks for the film.

## IV. RESULTS AND DISCUSSION

Three numerical tools (or modules) have been used to simulate the ice accretion over an airfoil. These three modules are FENSAP-ICE, DROP3D and ICE3D. These are state-of-the-art icing codes capable of 2D and 3D icing simulation for a large variety of applications. The flow field is simulated using a RANS [Reynold-Averaged- Navier-Stokes] flow solver, droplet and ice crystal impingement are simulated using an Eulerian approach; ice growth is captured by solving the partial differential equations (PDEs) on the iced geometry. Table 1 shows the reference conditions used for the simulation of ice accretion. The reference conditions could be changed depending upon the need of the study.

Table I. Reference conditions

| | |
|---|---|
| Characteristic length | 0.914 m |
| Air velocity | 100 m/s |
| Air static temperature | 262 K |
| Air static pressure | 101325 Pa |
| Reynolds number | $7.4136 \times 10^6$ |
| Mach number | 0.308 |
| Liquid Water Content(LWC) | 0.0007 kg/m$^3$ |
| Droplet diameter | 20 microns |
| Water density | 1000 kg/m$^3$ |

The airfoil taken for the study is NACA0012. The same has been used in almost all the literatures dealing with ice accretion [30]. The prediction of ice shape, thickness of ice and mass caught during the accretion has been attempted in this study. The extensive physical validation has been done with the experimental results obtained from NASA's icing wind tunnel as reported in Ref.[30]. Each module described above runs iteratively in a multi-step process. The selection of LWC is based upon the 14 CFR Part 25, Appendix C for continuous maximum icing conditions mentioned in FENSAP-ICE user manual.

Some of the key parameters such as free stream icing velocity, duration of icing, airfoil chord length, angle of attack(α) icing, liquid water content LWC, median volume diameter, ambient temperature and equivalent sand-grain surface roughness define the ice accretion process. Flight velocities are chosen according to typical cruise speeds of aircraft. All CFD calculations are performed by using a steady-state Spalart-Allmaras turbulence model and a streamline upwind artificial viscosity model.

In Fig.1 (a) is shown the contours of velocity magnitude and Fig. 1(b) show the pressure distribution around the airfoil. The results were produced from the first module: FENSAP, which is used for flow calculations. The angle of attack of the flow is zero degree and the stagnation point is at the leading edge (LE) of the airfoil. The maximum pressure observed at LE is $1.033 \times 10^5$ Pa [reference pressure is $1.01325 \times 10^5$ Pa] and the maximum velocity magnitude noted during the flow is 6.41 m/s

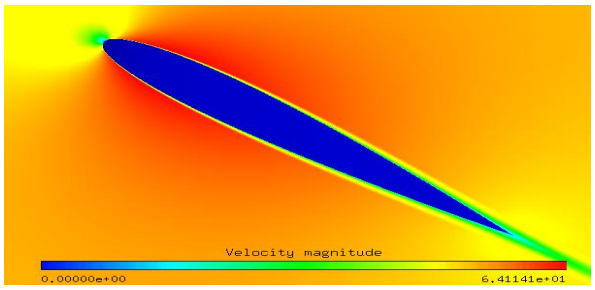


**Fig.1(a) Contours of velocity magnitude distribution around airfoil**

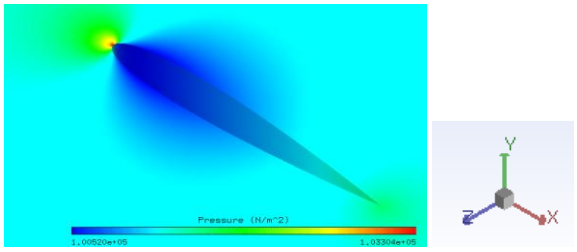


**Fig.1(b) Contours of pressure distribution around airfoil**

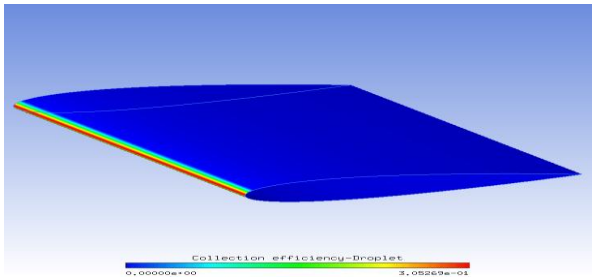


**Fig.2 (a) Contours of droplet LWC**

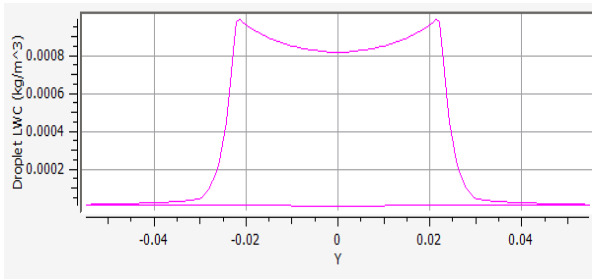


**Fig. 2 (b) Variation of droplet LWC in the LE**

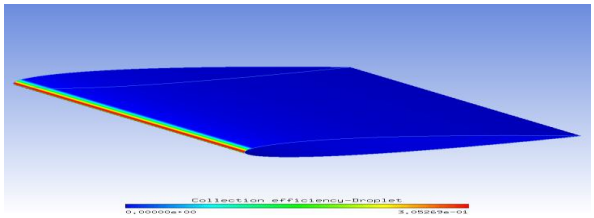


**Fig.3 (a) Contours of collection efficiency**

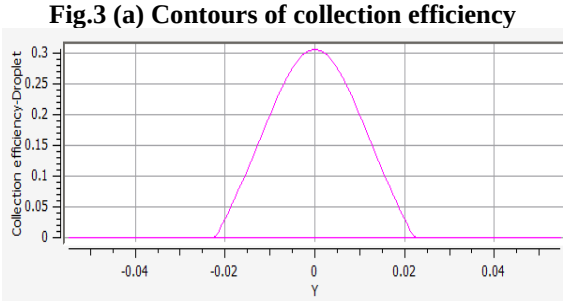


**Fig.3. (b) Variation of collection efficiency**

The Figs.2 (a)-(b) and Figs.3 (a)-(b) are showing some of the outputs of the second module: DROP3D. The Fig.2 (a) and (b) depict the LWC of droplet at the LE. More amount of droplet LWC (12.5% rise from the values of LWC at the middle and around 70% up from Y=+/- 0.04) is observed at the upper and lower portions of the LE which is clear in Fig. 2(b). Similarly the highest collection efficiency noted is 0.3 that is shown in Fig. 3(b). and the same is observed at the middle of LE (Y=0) as shown in Fig. 3(a). This is around 30% rise from the collection efficiency at Y=+/- 0.02.

In Fig. 4(a) is shown a cut plate across the airfoil where ice accretion has already begun at the reference conditions mentioned above. This is produced from the third module, that is, ICE3D. Fig.4 (b) shows the gridding arrangement [chosen from the three different grids used for icing simulation] with iced airfoil. The grid independence study has been carried with tolerance values of 10-10 for the convergence of each flow computed variable. The finer grids (1/5th of the size of the largest grid element used) were found near the areas of curvature: Leading Edge (LE) and Trailing Edge (TE) of NACA0012.

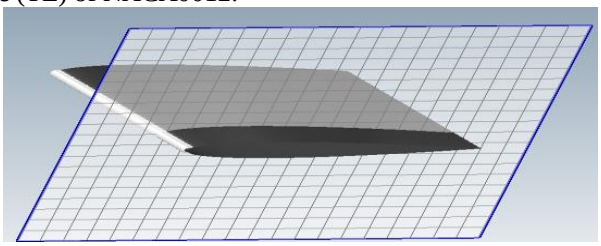

**Fig.4 (a) A cut plane shown across the LE of NACA0012**

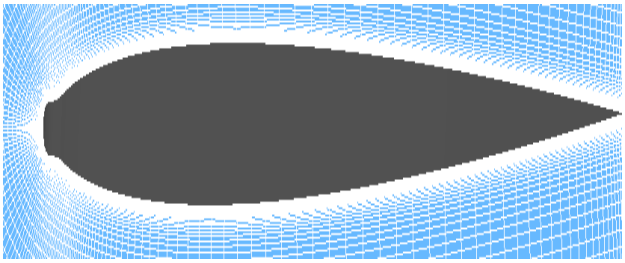

**Fig.4 (b) Close-up view of grid around the airfoil with ice accreted at LE**

Figs.5 (a)-(d) show the comparison of ice thickness with respect to the total time of accretion. The total time of accretion (tice) was changed in ICE3D solver and the mass of ice caught and thickness of ice over LE are observed.

Some typical cases have been presented below. For tice=5 min, the total mass of ice was 0.2 kg for tice=150 min, the total mass of ice was 5.6 kg. So, it is clear from these plots that the total time of accretion has strong linear correlation with the mass of ice accreted.

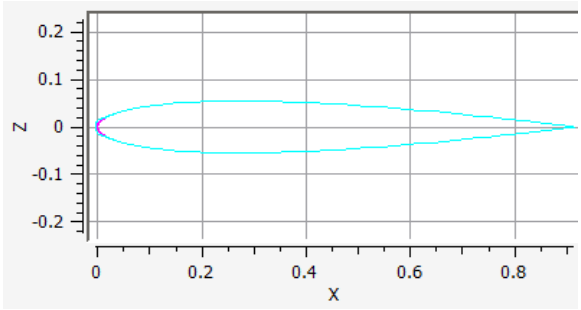


(a) Time of accretion = 5 min

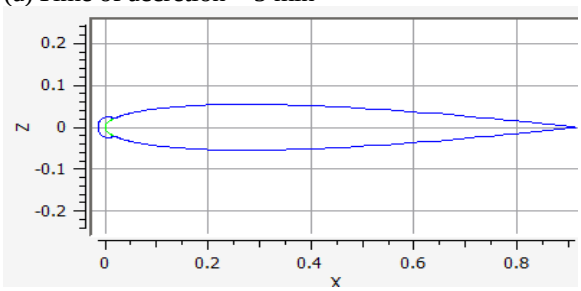


(b) Time of accretion = 40 min

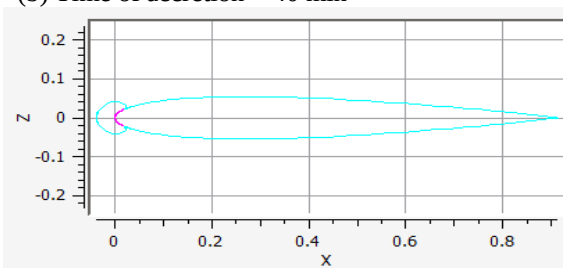


(c ) Time of accretion = 100 min

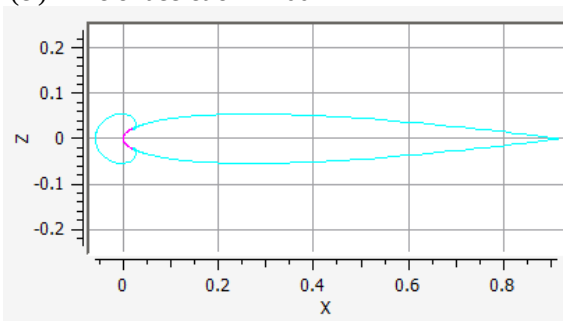


(d) Time of accretion = 150 min

Fig.5 Comparison of thickness of ice formed over airfoil with respect to time of accretion

Before

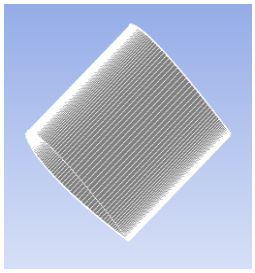

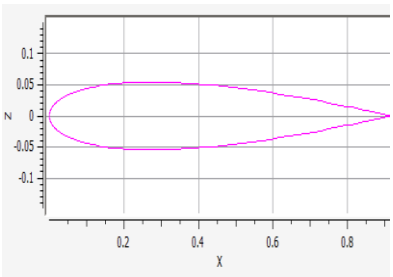


After

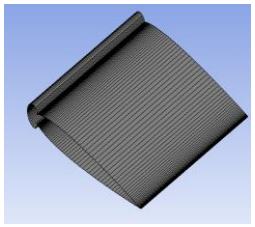

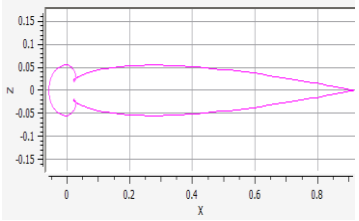


Fig.6 Comparison of NACA0012 airfoil before and after ice accretion at Reynolds number = $7.4x10^6$

After understanding the outputs from the fundamental equations used in the different solvers used in FENSAP-ICE system to achieve ice accretion and their interaction with each other through grid file, solution file and configuration settings it was decided to verify and validate the approach and the findings of research. In Fig.7(a) is shown a comparison of simulation results of coefficient of lift (CL) for the NACA0012 airfoil for different angles of attack(AOA) with experimental data published in Ref [30]. The matching is found to be fairly well and the same has also been observed in Fig.7 (b) that shows a comparison of simulation results of coefficient of drag (CD) for the NACA0012 airfoil for different angles of attack with experimental data published in Ref [30]. After these two verifications and validation of the approach it was decided to compare and verify the ice accretion in the LE.

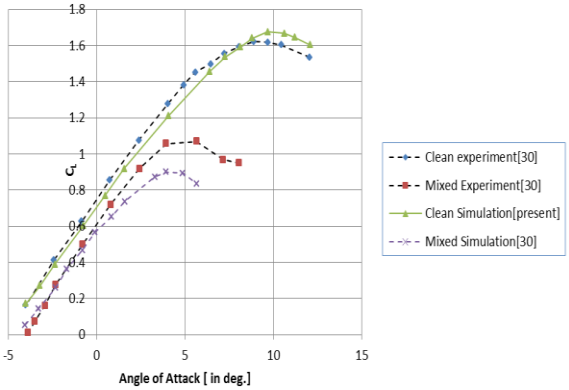


Fig. 7 (a) Comparison of simulation results of coefficient of lift (CL) for the NACA0012 airfoil for different AOA with experimental data, Ref [30]

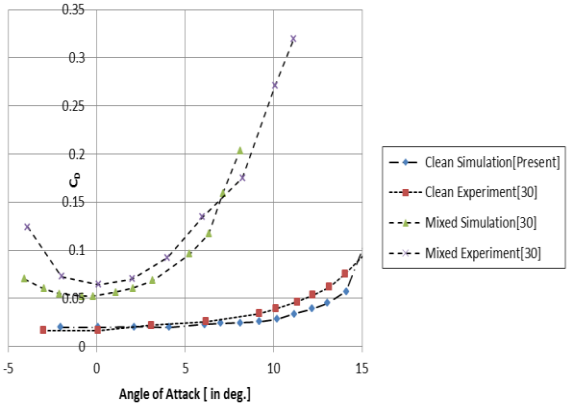


Fig.7 (b) Comparison of simulation results of coefficient of drag (CD) for the NACA0012 airfoil for different AOA with experimental data, Ref [30]

The correlation among AOA, coefficient of drag (CD) and coefficient of drag (CD) and coefficient of lift (CL) has been established and presented in Table 2. It shows a measure of the direction and strength of the relationship between two variables. It is measured by the Pearson's correlation coefficient(r) that varies between -1 and +1. For a positive association r > 0, for a negative association r < 0, if there is no relation r = 0. The closer r is to 0 the weaker the relationship and the closer to +1 or -1 the stronger the relationship; the sign of the correlation provides direction only. Correlation does not mean causation. A strong relationship between any two variables does not necessarily mean that one causes the other. From the table it is noted that AOA has a strong correlation with both CL and CD.

**Table II. Correlation Matrix**

| | AOA | CL | CD |
|---|---|---|---|
| AOA | 1.00 | 0.97 | 0.83 |
| CL | 0.97 | 1.00 | 0.68 |
| CD | 0.83 | 0.68 | 1.00 |

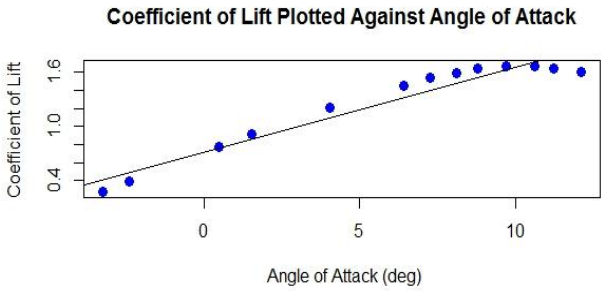


Fig. 8 Relation between coefficient of lift (CL) and AOA for clean simulation

The best fit line (regression line obtained after linear regression was done) runs from 0.4 to 1.6 linearly for increasing values of AOA in Fig.8. Fig.9 depicts the fitted values of CL versus residuals where CL is the response. All the fitted values are surrounded and changing around the regression line with very minimum residuals (variations are the least) and only two readings of CL are outliers and hence these are not considered for the study.

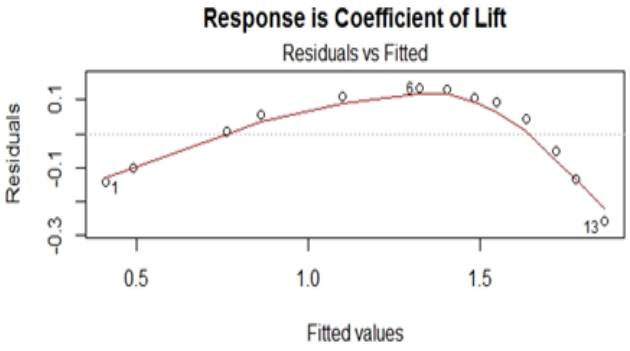


Fig.9 Best fit of coefficient of lift (CL) versus residuals for clean simulation

From Fig.10 it is observed that the best fit line (regression line obtained after linear regression was done) starts from a value lesser than 0.02 and ends around 0.04 linearly for increasing values of AOA. Fig.11 shows the fitted values of CD versus residuals where CD is the response. All the fitted values are bouncing around the regression line that has the minimum residuals (variations around it are the least) and only three readings of CD are outliers and hence these three values are out from the consideration in the study.

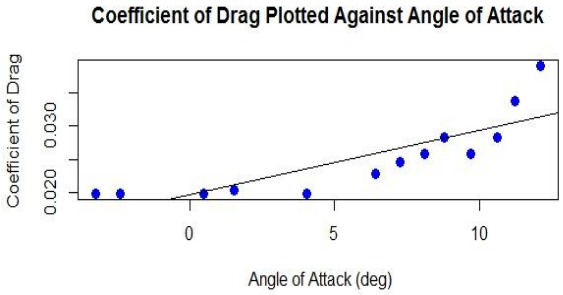


**Fig. 10 Coefficient of drag (CD) versus AOA for clean simulation**

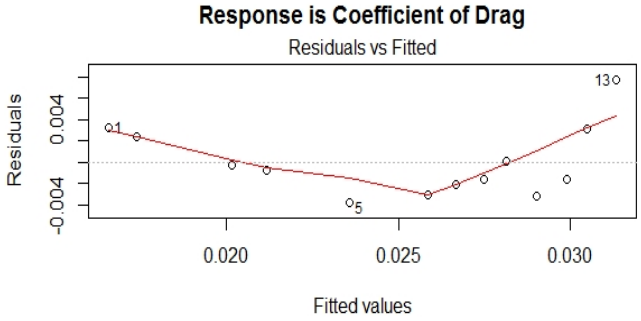


**Fig.11 Best fit of coefficient of drag (CD) versus residuals for clean simulation**

In Fig.12 is shown a comparison of simulation of ice accretion for the NACA0012 airfoil with experimental data published in Ref [30]. Though there is a good matching of the trend of ice, obtained from simulation, with the experiment the exact amount of ice or thickness does not match with that of the experiment. However, the physical validation of numerically obtained values of icing geometry has been accomplished with the geometry predicted during experiment, mentioned in Ref [30], conducted in icing wind tunnel.

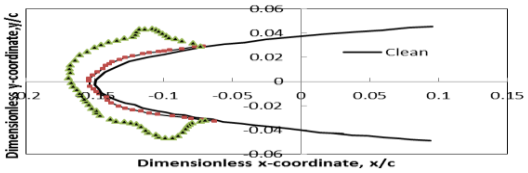


**Fig. 12 Comparison of simulation of ice accretion for the NACA0012 airfoil with experimental data, Ref [30]**

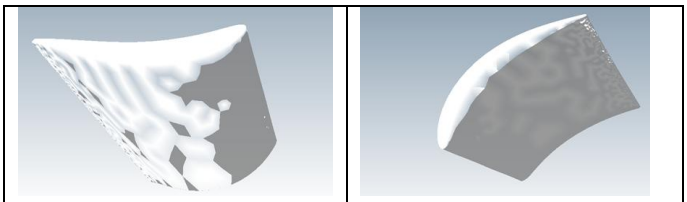

(a) Ice on surface of a fan blade

(b) Ice over the airfoil portion

**Fig.13 Accumulation of ice on surface of a fan blade used in the study post the validation**

The same reference conditions as described above for NACA0012 have been used for the fan blade. The visual inspection of the two figures shows that the thickness of ice varies over the surface and the mean thickness over the airfoil section is around 25% higher than that over the entire blade surface.

## V. CONCLUSION

Before The simulation of ice accretion for NACA0012 airfoil has been carried out. The three modules of FENSAP-ICE have been used to simulate the ice accretion process over the airfoil surface. It is found from the simulation and validation that the total time of ice accretion has a significant impact on the mass of ice formed and ice accreted. The study also revealed the accretion has been affected by AOA. It is found that the total time of accretion has a strong linear correlation with the mass of ice accreted. The regression analysis also revealed that the strong linear relationship between AOA and CL and CD. The CL (the best fit values) varies from 0.4 to 1.6 and CD (its best fit values) runs between 0.02 and 0.04. The correlation matrix has established and exposed the fact that there is a strong correlation of AOA with both CL and CD during icing. It is also found from the study that the icing has reduced the CL and lowered stall angle. AOA and time of accretion are some of the key variables that would be studied in future to understand their effects in ice accumulation and accretion phenomenon for cascade of blades with cambered airfoils.

## ACKNOWLEDGMENT

We thank all the faculties of Aeronautical department, Acharya Institute of Technology for sharing their pearls of wisdom & motivated us during the course of this research.

## REFERENCES

1. T. P. Meshcheryakova, Design of Systems of Protecting Aircraft and Helicopters [in Russian], Mashinostroenie, Moscow (1977).
2. M. B. Bragg, Aircraft aerodynamic effects due to large-droplet ice accretions, AIAA 34th Aerospace Sciences Meeting, Reno, NV, January 15–18, AIAA Paper, No. 0932 (1996).
3. S. Dutch, Natural and Applied Sciences. http://www.uwgb.edu/dutchs/EarthSC102Notes/102Clouds.htm.
4. M. Potapczuk, Numerical analysis of a NACA 0012 airfoil with leading edge ice accretions, AIAA Paper, No. 0101 (1987).
5. A. A. Prikhod′ko, Computer Technologies in Aerohydrodynamics and Heat/Mass Transfer [in Russian], NaukovaDumka, Kiev (2003).
6. S. C. Caruso, Development of an unstructured mesh/Navier–Stokes method for aerodynamics of aircraft with ice accretions, AIAA Paper, No. 0758 (1990).
7. S. C. Caruso and M. Farshchi, Automatic grid generation for iced airfoil flowfield predictions, AIAA Paper, No. 0415 (1992).
8. J. Dompierre, D. J. Cronin, Y. Bourgault, et al., Numerical simulation of performance degradation of ice contaminated airfoils, AIAA Paper, No. 2235 (1997).
9. S. Lee and M. B. Bragg, Effects of simulated spanwise ice shapes on airfoils: experimental investigation, AIAA Paper, No. 0092 (1999).
10. S. Lee, H. S. Kim, and M. B. Bragg, Investigation of factors that influence iced airfoil aerodynamics, AIAA Paper, No. 0099 (2000).
11. H. S. Kim and M. B. Bragg, Effect of leading-edge ice accretion geometry on airfoil aerodynamics, AIAA Paper, No. 3150 (1999). 606
12. T. Dunn and E. Loth, Effects of simulated spanwise ice shapes on airfoils: computational investigation, AIAA Paper, No. 0093 (1999).
13. S. Kumar and E. Loth, Aerodynamic simulations of airfoils with large-droplet ice shapes, in: Proc. 38th Aerospace Sci. Meeting and Exhibit, Reno NV, AIAA Paper, No. 0238 (2000).
14. A. Baumert, S. Bansmer, P. Trontin, P. Villedieu, Experimental and numerical investigations on aircraft icing at mixed phase conditions, International Journal of Heat and Mass Transfer, Volume 123, Pages 957-978 (2018)
15. S. V. Alekseenko, Numerical Simulation of the Processes of Hydrodynamics and Heat/Mass Transfer in Regions with Free Boundaries, Candidate′s Dissertation (in Engineering), Dnepropetrovsk (2012).
16. 18. A. A. Prikhod′ko and S. V. Alekseenko, Mathematical simulation of the processes of heat and mass transfer in the icing of airfoils, in: Proc. 6th Minsk Int. Heat Mass Transfer Forum "MIF–VI," ITMO im. A. V. Luikova NANB, Vol. 1, Minsk (2008), pp. 1–10.
17. 19. A. A. Prikhod′ko and S. V. Alekseenko, Icing of airfoils. Simulation of an air–drop flow, Aviats.-Kosm.Tekh.Tekhnol., No. 4, 59–67 (2013).
18. G. Fortin, J. Laforte, and A. Beisswenger, Prediction of ice shapes on NACA 0012 2D airfoil, Anti-Icing Mater. Int. Lab., No. 2154 (2003).
19. Fortin G., Ilinca A., and Brandi V. A new roughness computation method and geometric accretion model for airfoil icing. J. Aircraft., 41, No. 1, 119–127 (2004).
20. B. L. Messinger, Equilibrium temperature of an unheated icing surface as a function of airspeed, J. Aeronaut. Sci., 20, No. 1, 29–42 (1953).
21. F. H. Lozowski, J. R. Stallabras, and P. F. Hearty, The icing of an unheated nonrotating cylinder in liquid water droplet ice crystal clouds, National Research Council, Laboratory report No. LTR-LT-96 (1979).
22. Ice Accretion Simulation, AGARD-AR-344, Hull (1997).
23. W. B. Wright, User's manual for the improved NACA lewis ice accretion code LEWICE 1.6, Contractor Report NACA, May, 1995.
24. P. Louchez, G. Fortin, G. Mingione, and V. Brandi, Beads and rivulets modeling in ice accretion on a wing, in: Proc. 36th Aerospace Sci. "Meeting & Exhibit," American Institute of Aeronautics and Astronautics, Reno, Nevada (1998).
25. F. H. Ludlam, The heat economy of a rimed cylinder, Q. J. R. Meteor. Soc., 77, No. 1, 663–666 (1951).
26. A. P. Broeren, E. A. Whalen, and G. T. Busch, Aerodynamic simulation of runback ice accretion, J. Aircraft, 47, No. 3, 1641–1651 (2010).
27. ANSYS® FENSAP-ICE User Manual, Release 18.2,Ansys, Inc.
28. Wagdi G. Habashi et. al, Development Of A Second Generation In-Flight Icing Simulation Code, Journal of Fluids Engineering, American Society of Mechanical Engineers, 2006, 128 (2), pp.378-387
29. P. Trontin, P. Villedieu. A comprehensive accretion model for glaciated icing conditions. International Journal of Multiphase Flow, Elsevier, 2018, pp.1-10.
30. Hann, R., Brandrud, L., Kroegenes, J., Bartl, J., Bracchi, T., and Saetran, L., "Aerodynamic Performance of the NREL S826 Airfoil in Icing Conditions at Low Reynolds Numbers," Unpublished manuscript.
31. V. Kashevarov, A & L. Stasenko, A. (2018). Modeling of Ice Accretion on the Airfoil Surface in an Air Flow Containing Ice Particles. Journal of Applied Mechanics and Technical Physics. 59. 645-652.

## AUTHORS PROFILE

Ms. Swetha S is currently as assistant professor in the department of Aeronautical Engineering, Acharya Institute of Technology. She obtained her M.Tech and B.E degrees from the department of Mechanical Engineering. She is a life member of ISTE. She got 8+ years of teaching experience with 7+ publications in different journals and conferences.

Dr. Abdul Sharief is currently professor and principal, dept. of Mechanical Engineering, PA College of Engineering. He obtained his degrees from the department of Mechanical Engineering. He is a life member of ISTE. He has got 25+ years of teaching experience with 20+ publications in different journals and conferences.

Dr. SK Maharana is currently professor and head of Aeronautical Engineering, Acharya Institute of Technology. He obtained his M.Tech and PhD degrees from the department of Aerospace Engineering, IIT Kharagpur. He is a life member of ISTE and ISWE. He has worked in one of the most admired aviation industries and has got 13 years of teaching experience with 35+ publications in different journals and conferences.